Field and theoretical dynamic response of vertically loaded helical and driven steel piles

Mohamed Elkasabgy, Researcher, P.Eng.
M. Hesham El Naggar, Professor and Associate Dean, Ph.D., P.Eng.
Dept. of Civil Eng., University of Western Ontario, London, ON, Canada
M. Sakr, PhD., P.Eng.,
WorleyParsons, Edmonton, Canada

ABSTRACT
This paper presents the comparison between the full-scale vertical vibration response of a 9.0 m large-capacity single-helix pile and a driven steel pile of similar length, in order to qualify and quantify the large-capacity helical piles and driven piles' dynamic performance. The test piles were close-ended piles with shaft outer diameter of 324 mm and helix diameter of 610 mm. Quadratic type harmonic load tests were conducted using five force intensities applied within frequency range that covered the resonance frequencies of the tested pile-soil-cap systems. The acceleration at the level of the centre of gravity of the pile cap system was recorded. The dynamic and static properties of the site soils were determined using the conventional soil boring and testing methods and the seismic cone penetration tests. The current study compares the field observations against the theoretical predictions and provides an insight into the role of pile-soil interaction in theoretically matching the field observations. The effects of soil nonlinearity, soil separation, pile slippage, and the effect of the boundary zone concept were considered in the simulation process and the stiffness and damping parameters of the test piles were obtained. The findings from this project are considered to be useful in the design and analysis of piles under similar geometrical and material conditions as well as validating the adequacy of the existing theoretical formulations for analysing the dynamic response of helical piles.

RÉSUMÉ
Cet article présente la comparaison entre la réponse vibratoire vertical à grande échelle d'une pile 9,0 m de grande capacité unique hélice et un pieu en acier mécanique de longueur similaire, afin de qualifier et de quantifier la grande capacité pieux hélicoïdaux et des pieux enfoncés «dynamique performance. Les pieux d'essai ont été fermées pieux de diamètre extérieur de 324 mm arbre et le diamètre d'hélice de 610 mm. Essais de type quadratique charge harmonique ont été menées en utilisant cinq intensités force appliquée dans la plage de fréquence couverte les fréquences de résonance des systèmes de pile-sol-plafond testé. L'accélération au niveau du centre de gravité du système de plafonnement des tas a été enregistré. Les propriétés statiques et dynamiques des sols du site ont été déterminés en utilisant le sol classique ennuyeux et méthodes d'essais et les tests de pénétration au cône sismique. La présente étude compare les observations sur le terrain contre les prédictions théoriques et donne un aperçu du rôle de l'interaction pieu-sol correspondant à la théorie des observations de terrain. Les effets de la non-linéarité du sol, la séparation du sol, de glissement de pieux, et l'effet de la notion de zone frontière ont été pris en compte dans le processus de simulation et de la raideur et de l'amortissement des pieux d'essai ont été obtenus. Les résultats de ce projet sont considérés comme utiles dans la conception et l'analyse des pieux dans les mêmes conditions géométriques et des matériaux ainsi que de valider la pertinence des formulations théoriques existantes pour l'analyse de la réponse dynamique des pieux hélicoïdaux.

1 INTRODUCTION

Helical piles are used as a foundation system for several engineering applications. Helical piles can be manufactured in different geometrical configurations with a wide variety of shaft diameters. The use of large-capacity (or large diameter helical piles) offer a significant advantage for applications involving static loads. Helical piles have a variety of advantages over conventional foundation types such as driven steel piles. They can be easily installed using minimal equipment, removed, and reused. Furthermore, they allow immediate loading upon installation. Additionally, in the case of high ground water level, helical piles save dewatering and/or pumping of the construction site (Bobbitt and Clemence 1987).

Helical piles are mostly designed to sustain static loading especially for uplift loads and seismic loading conditions. Such applications include: transmission towers, pipelines, and supporting retaining structures (Adams and Klym 1972; Carville and Walton 1995; Zhang 1999; El Naggar and Abdelghany 2007a,b). Recently, the use of helical piles has gained popularity, especially large-capacity helical piles, to provide superior resistance to compression static axial loads and machine foundation dynamic loads (Sakr 2009; Elkasabgy *et al*. 2010)

Piles are commonly employed to support foundations that are subjected to dynamic loads. The dynamic response of these foundations depends on the dynamic stiffness and damping of the piles, which is affected by the pile-soil interaction. Many theoretical studies have been conducted in order to estimate the dynamic impedances and performance of piles. The theoretical approaches include: the lumped mass model (Penzien 1970), the Winkler approach (El Naggar *et al*. 2005), the finite element methods (Kuhlemeyer 1979; Manna and Baidya 2009), the cone model by Wolf *et al*. (1992), and the plane strain solution, which is based on the continuum approach (Novak, 1974; Novak, 1977; Nogami and Novak, 1976; and Novak and El Sharnouby, 1983).

The plane strain approach accounts for soil-pile interaction and energy dissipation through elastic wave propagation in the soil continuum. Novak and Aboul-Ella (1978a, 1978b) extended the theoretical solutions for piles embedded in layered soils. Novak and Sheta (1980) introduced the concept of soil weak boundary zone around the piles to account for soil nonlinearity and pile-soil slippage, separation, and lack of bonding.

The published literature on experimental data of vertical dynamic performance of piles is limited. Blaney *et al*. (1987) conducted a full-scale large-amplitude vertical vibration test on a group of nine driven piles and two single piles, while two groups of concrete and steel piles were tested in field by El Marsafawi *et al*. (1992) to validate the available linear theories. On the other hand, Novak and Grigg (1976), Sheta and Novak (1982), and El Sharnouby and Novak (1984) conducted field small-scale vibration tests on groups of piles installed in silty sand soil.

The dynamic design of piles, including helical piles, requires adequate evaluation of their impedance characteristics. This necessitates a proper understanding of the load transfer mechanism between the pile shaft and helix, and the surrounding soil during dynamic loading.

2 OBJECTIVES

The main objectives are to investigate the performance of single large-capacity helical and driven piles under quadratic vertical vibrations in order to reach a formulation for estimating the stiffness and damping characteristics of helical piles. Both full-scale field tests and theoretical approaches are incorporated. Consequently, the computer program DYNA 6 is adopted to estimate the response curves and load transfer mechanism of the test piles and compare them with the field measured curves.

3 SITE CHARACTERISTICS

The test site is located in Ponoka County, 12 km north of the town of Ponoka in the Central Alberta region, Canada. Standard penetration tests (SPT) were performed in the borehole to determine the *N* values, and laboratory tests were conducted on disturbed and undisturbed samples extracted from the borehole. In addition, dynamic in-situ tests, consisting of three seismic cone penetration tests (SCPT), were carried out to a depth of 15.0 m in order to determine the profile of the shear and compression wave velocities, V_s and V_p. Figure 1 illustrates the locations of the test piles, SCPT sounds, and the augered borehole.

Based on the soil investigation program, the soil profile at the location of the test piles consists of a 1.3 to 1.5 m thick silty to sandy silt crust with some organic materials. The crust is underlain by a 3.0 m stiff layer of brownish clay to silty clay and clayey silt with medium compressibility, which interbedded with seams of silt. It is followed by interbedded layers of very stiff grey silty clay, clayey silt, and clay of thickness 1.3 m, which is underlain by a dense to very dense silty sand/sand to sandy silt layer of thickness 0.5 m. Underneath it, there is a 7.2 m thick layer of very stiff to hard grey clay till, with low to medium compressibility, overlays interbedded layers of sandy silt, silt, clayey silt, and silty clay. The ground water level was established at 1.2 m below the ground surface.

The distribution of shear wave velocity, V_s, was obtained from the measurements of the SCPT and from the established empirical correlations in terms of *N* values. The values of the small-strain undrained Poisson's ratio, ν, were obtained from the V_s and V_p measurements, and was found to vary between 0.35 and 0.49. Finally, the shear modulus, G_o, of the soil was determined using the elastic theory, $G_o=\rho(V_s)^2$, where ρ is the mass density of soil. Figure 2 presents the variation of the small-strain dynamic properties, bulk unit weight, γ, moisture content, W_c, and specific gravity, G_s, of the site soils.

4 EXPERIMENTAL SETUP

The helical pile was 9.0 m long pile with outer steel pipe shaft diameter of 0.324 m, and a single helix with a diameter of 0.61 m. The pile was closed-ended with a flush closure steel plate. The pile was installed into the site soil by applying a clockwise turning moment (torque) to the pile shaft, by a hydraulic torque head, while sustaining a constant rate of penetration of one helix plate pitch (152.4 mm) per revolution. The unsupported pile length protruded 0.6 m above the ground surface. The driven pile was closed-ended, of similar geometrical configurations. The test piles had Young's modulus of 210 GPa. To ensure that the resonance frequencies were well defined and within the frequency range of the exciting machine, a steel test body was added on the cap of each of the test piles. The test body comprised of 59 machined circular steel plates. The schematic diagram of the experimental setup is shown in Fig. 3. The vertical excitation force was produced by a Lazan mechanical oscillator mounted over the test body mass. The oscillator was driven by a motor capable of generating sinusoidal force of 23.5 kN peak-to-peak, through a well-balanced flexible drive shaft. The full test setup and test piles description is provided in Elkasabgy *et al*. (2010).

The vibration measuring apparatuses consisted of two uniaxial piezoelectric accelerometers, one triaxial accelerometer, and frequency measurement unit to monitor excitation frequency. In order to obtain the strain and force distribution along the helical pile, half-bridge strain gauge circuits were affixed on the inner surface at specified locations. Each level of gauges encompassed four half bridges allocated equidistantly (Fig. 4).

5 VERTICAL DYNAMIC RESPONSE OF PILES

The dynamic experiments were conducted on the helical and driven piles two weeks after installation, when the soil around pile's shaft was disturbed because of the installation process. Initially, the oscillator was operated at low-force level (low excitation intensity) in order to keep the vibration amplitudes small enough to avoid any initial pile-soil separation and strong nonlinearity. The oscillator

covered a frequency spectrum from about 3 to 60 Hz. The steady-state acceleration time history was recorded after reaching equilibrium by stopping at each frequency.

For the adopted static mass, 4849.5 kg including the weight of cap, test body, and oscillator, tests were conducted at five different excitation intensities ($m_e.e$ = 0.091, 0.12, 0.16, 0.18, and 0.21 kg.m) for the helical pile and three intensities (0.091, 0.16, and 0.21 kg.m) for the driven pile. The excitation intensities are provided in terms of $m_e.e$ in which m_e and e are the oscillator eccentric rotating masses and the eccentricity of the rotating masses, respectively. The magnitude of the dynamic force generated at the pile head is related to the excitation intensity of the oscillator and the measured acceleration by $m_e.e.\omega^2.sin\omega t+m.a$, where ω is the circular frequency, a is the measured acceleration at the centre of gravity of the cap-test body-oscillator assembly, and m is the static mass. The steady state dynamic response to the induced vertical excitation was measured over the oscillator frequency range.

The typical measured vertical vibration response curves for both of the helical and driven piles are presented in Fig. 4. The vertical displacements of piles

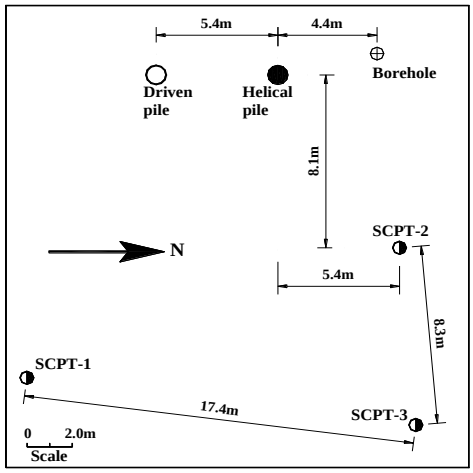

Figure 1. Locations of piles, SCPT, and borehole

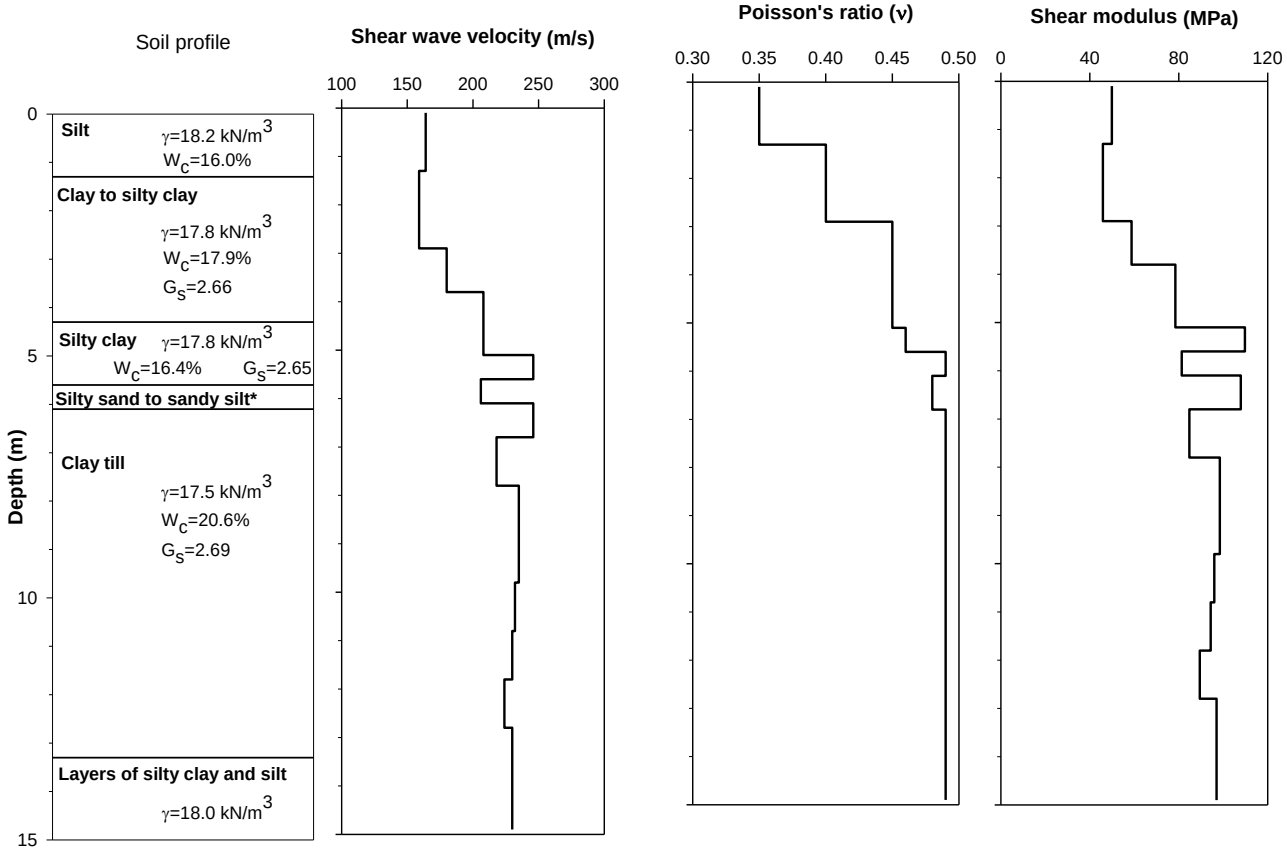

* Silty sand layer: γ=18.8 kN/m^3; W_c=20.9%; and G_s=2.68

Figure 2. Measured dynamic and index properties

vary with single resonant peak for both piles. The maximum displacements measured at the centre of gravity of the static mass are 0.32 mm for the helical pile and 0.31 mm for the driven pile.

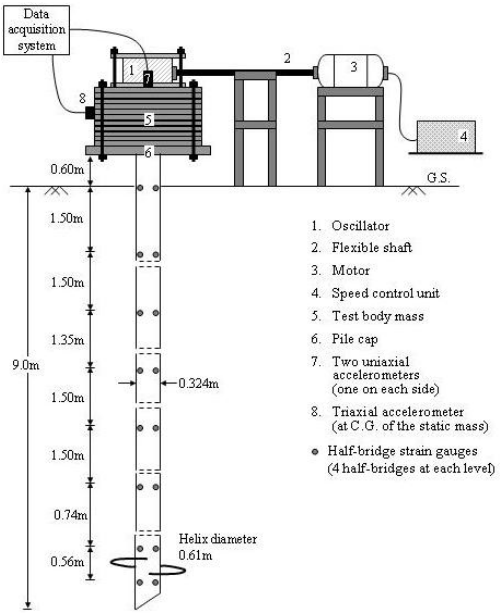

Figure 3. Test setup

The maximum displacements measured at the centre of gravity of the static mass are 0.32 mm for the helical pile and 0.31 mm for the driven pile. These amplitudes reflect the moderate level of applied vertical vibration. It is worth noting that the response of the driven pile was very close to that of the helical pile. This indicates that most of the soil reactions to dynamic vibration were developed along the pile shaft, as explained later in the paper. The observed differences in amplitudes may be ascribed to the variation of soil profile surrounding the pile and/or the extent to which the soil was disturbed around the pile during installation.

Figure 5 shows the dimensionless response curves of the test piles. The dimensionless amplitudes are defined as:

$$R_d = \frac{m}{m_e.e}.V \qquad [1]$$

where V is the measured vertical amplitude. For linear vibrating system, all dimensionless curves shown in each figure should coincide and the amount by which they differ represents the degree of nonlinearity in response. For the helical pile, slight nonlinearity is observed, where the measured resonant amplitude shifts from 32 to 30 Hz. This indicates a reduction in stiffness - proportional to square of frequency - to almost 88 % of the highest value associated with the lowest excitation intensity.

6 THEORETICAL ANALYSIS

The response of piles to dynamic loads is affected by the interaction between the piles and the surrounding soil, which generates geometrical damping and hysteretic damping. Two different theoretical continuum approaches were adopted to investigate the performance of both of the helical pile and driven pile under vertical vibration. The two approaches are incorporated in the program DYNA 6 (El Naggar *et al*., 2011). The analysis includes the estimation of the response curves, dynamic load in piles, and stiffness and damping of the pile-soil system.

6.1 Linear Approach

The theoretical approach was presented by Novak and Aboul-Ella (1978a, 1978b) using the plane strain condition as an extension of the elastic solution provided by Baranov (1967) and Novak (1974, 1977). The approach was derived to obtain the stiffness and damping of piles in layered soil. The approach adopts the following assumptions: (1) the soil is composed of horizontal linearly viscoelastic layers with material damping; (2) the pile is elastic and divided into finite elements, each of the same length as the side soil layer; and (3) the soil below the pile tip is a viscoelastic half-space. The soil reaction along the pile shaft was provided in the form of complex soil stiffness by Novak *et al*. (1978), as in Eq. 2. Veletsos and Verbic (1973) presented the soil reaction at pile toe (Eq. 3):

$$K_{vs} = G_{os}\left(S_{v1} + S_{v2}\right) \qquad [2]$$

$$K_{vs} = G_{ot}.R_t\left(S_{Cv1} + iC_{v2}\right) \qquad [3]$$

in which G_{os} and G_{ot} are the shear modulus of soil along pile shaft and tip, respectively; R_t is the pile tip radius; S_{v1} and S_{v2} are the real and imaginary parts of the dimensionless complex soil stiffness along pile shaft, respectively; and C_{v1} and C_{v2} are the real and imaginary parts of the dimensionless complex soil stiffness at pile toe. With harmonic motion having complex amplitude, the complex and frequency dependent impedance at the pile head is expressed as:

$$K_V = k_{V1} + ik_{V2} \qquad [4]$$

where k_{v1} and k_{v2} are the dynamic stiffness and damping impedances. The notation k_{v2} is equivalent to $\omega.c$ where c is the equivalent viscous damping coefficient that account for geometric and hysteretic damping.

In this analysis, no weak zone around the pile was considered and the value of the damping ratio of soil was assumed constant, 5 %, with depth. The soil beneath the tip of the helical pile - beneath the idealized helix - was assumed homogeneous with average shear modulus that represents the undisturbed soil beneath the upper and lower helices. The estimated response assuming no change of soil properties due to installation are compared with the measured response curves in Fig. 4. It can be noted that there is a significant difference between the estimated and measured response curves. The natural frequencies estimated from the linear approach are much higher than the measured values, by an average of 63 to 74 % for the helical pile and by 79 % for the driven pile. In addition, the estimated resonant peaks are more rounded, indicating higher damping compared to the

experimental results. This is also indicated in terms of much lower estimated vibration amplitudes compared with the measured values.

These discrepancies are because the soil adjacent to the test piles was disturbed during installation. Such disturbance is confined to an annular zone around the pile, which leads to reduced soil shear modulus and imperfect contact at the pile-soil interface. These effects are not accounted for when considering the linear approach. Ignoring soil disturbance in the analysis leads to overestimating the resonant frequency and damping and underestimating the resonant amplitude. With the passage of time, the soil regains its strength and eventually the expected behaviour matches that determined considering the linear soil conditions.

The disturbance occurred around the helical pile is believed to be highly significant. This is attributed to the nature of structured cemented silty clay/clayey silt soils of the test site. The installation disturbance destroyed the cementation between the soil particles, and it seems that this cementation requires long time to be re-established. Similar effects are expected to occur for the driven pile due to the disturbance associated with the driving process. O'Neill (2001) recommended that the capacity of driven piles in silty clay and clayey silt be reduced by 50 % because of the installation effects. He theorized that due to the propagation of stress waves during pile driving, the pile shaft vibrates, pushing the soil away from the shaft and thus reducing the contact surface (imperfect bonding between pile and soil). This level of disturbance is not expected to occur in sandy soils or purely cohesive soils. Consequently, the linear approach is not considered the ideal methodology to predict the vertical vibration response of helical and driven piles.

6.2 Nonlinear Approach

It is known that the pile performance is affected by the remoulding of soil around the pile during installation, nonlinearity of soil at the zone of high strain, lack of bond at the pile-soil interface, slippage, and separation. In order to account for most of these factors, Novak and Sheta (1980) extended the plain strain theory, explained previously, to assume that the pile is surrounded by a linear viscoelastic medium composed of two zones: an outer zone and an inner cylindrical weakened boundary zone surrounding the pile, as presented in Fig. 6. Soil disturbance and nonlinearity, weakened bond, and slippage are accounted for by a reduced shear modulus and increased material damping of the weakened boundary zone of soil.

As well be shown later, the parameters making up the properties of the weakened zone, including the shear modulus ratio, G_m/G_o, damping ratio, D_m, thickness, t_m, and mass participation factor (M.P.F) assigned to represent the percentage of weak zone soil mass vibrating in-phase with the pile, play an appreciable role in the overall dynamic response of the piles.

The complex soil reactions of the composite medium were developed by Novak and Sheta and substituted into the approach presented by Novak and Aboul-Ella (1978a) to calculate the complex and frequency dependent stiffness and damping constants of the piles, as follows:

$$K_{vm} = k_{vm1} + ik_{vm2} = \frac{E_p A}{R}\left[f_{vm1} + i\frac{\omega R}{V_t} f_{vm2}\right] \qquad [5]$$

where K_{vm} is the total stiffness of pile in the composite medium; k_{vm1} and k_{vm2} are the stiffness and damping impedances; f_{vm1} and f_{vm2} are the dimensionless stiffness and damping parameters; E_p and A are the modulus of elasticity and cross sectional area of the pile; and V_t is the shear wave velocity near pile tip. It is worth mentioning that the approach does not account for pile-soil separation near ground surface, which instead, could be modeled in DYNA 6 as a void soil layer with G_o=0.

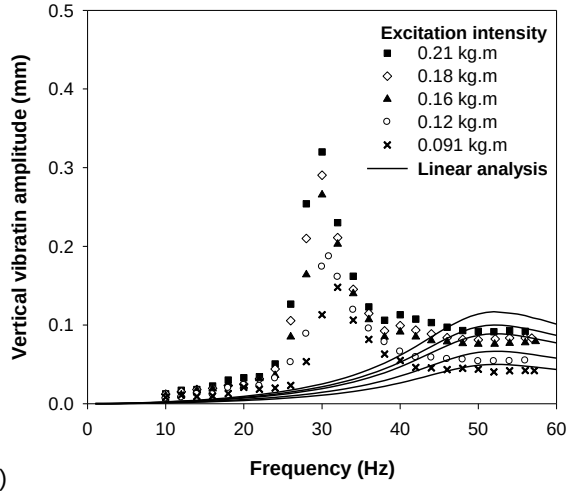

a)

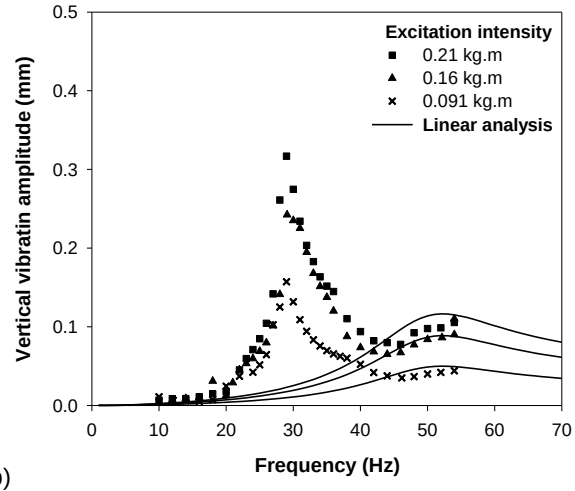

b)

Figure 4. Experimental versus linear approach response curves: a) helical pile and b) driven pile

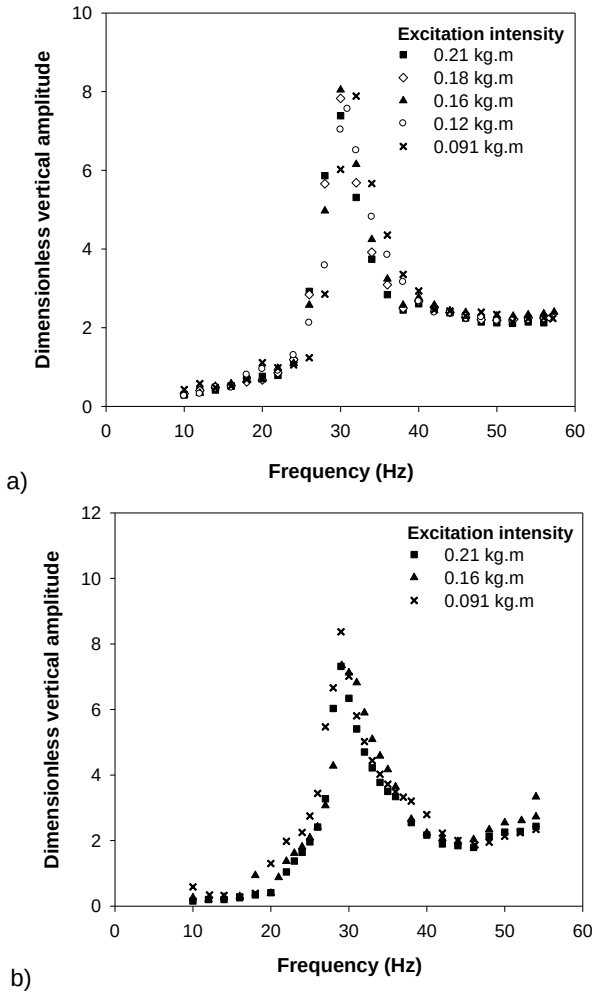

Figure 5. Dimensionless vertical amplitude: a) helical pile and b) driven pile

To properly estimate the behaviour of test piles considering the effects of soil disturbance, soil nonlinearity, and pile-soil separation, the nonlinear approach is adopted to account for radial soil inhomogeniety. The soil parameters in the weak boundary zone were adjusted to reach a reasonable match between the estimated and measured response curves. For different excitation intensities, the characteristics of the weak zone parameters are given in Fig. 6 and Table 1. As the excitation intensity increases, the shear modulus ratio, G_m/G_o, is reduced whereas the material damping ratio, D_m, is increased. This can be observed in the case of helical pile where slight to moderate soil nonlinearity is monitored. The variation of G_m/G_o is assumed to increase with depth, but D_m decreases with depth.

The weak zone's Poisson's ratio, ν_m, is taken 0.3 and constant with depth. The ratio of weak zone thickness to pile shaft radius, t_m/R, is presumed constant with depth, with a value of 1.2 for both test piles. It is believed that the zone where most soil disturbance occurs around driven piles installed in clayey soils extends 1 to 2 times pile radius around the pile, as per the soil disturbance and changes in state of stresses and pore pressure monitored in previous work by Randolph *et al*. (1979). A mass participation factor, M.P.F., of 0.25 is added for both the helical and driven piles. On the other hand, the properties of the soil medium surrounding the weak zone are similar to those given in the linear approach. Since the level of applied excitation was slight to moderate, it was considered that the pile separation developed mainly during piles installation. However, obtaining reliable values for pile-soil separation by physical measurements at ground surface was difficult. A trial-and-error technique was employed in the analysis and different separation values, l, were adopted until reaching the optimum. A ratio of $G_m/G_o = 0$ is assigned for the top most layer to account for the pile-soil separation in the analysis. The estimated depth of separation ranges between 1.54R (0.25 m) and 1.85R (0.3 m) for the test piles.

Table 1. Nonlinear approach parameters.

	Helical pile			**Driven pile**		
$m_e.e$ (kg.m)	l (m)	M.P.F	D.S.F	l (m)	M.P.F	D.S.F
0.091	0.30	0.25	1.0	0.30	0.25	1.02
0.12	0.30	0.25	1.0	-	-	-
0.16	0.30	0.25	1.0	0.30	0.25	1.02
0.18	0.25	0.25	1.0	-	-	-
0.21	0.20	0.25	1.0	0.30	0.25	1.02

The estimated response of the test piles using the nonlinear approach are plotted versus the experimental results in Fig. 7. It can be observed that there is a favourable agreement between the measured and estimated responses using the nonlinear approach. It can be concluded that incorporating the weak boundary zone and pile-soil separation in the model enabled capturing the real vertical vibration performance of helical and driven piles by providing excellent prediction of resonant frequencies, amplitudes, and damping, compared to the predicted values by the linear approach.

7 STIFFNESS AND DAMPING

The theoretical vertical stiffness and damping, predicted from the linear and nonlinear approaches, for the test piles are shown in Figs. 8 and 9. It can be observed that the linear approach highly overestimates both the stiffness and damping of piles, with no variation in the stiffness and damping characteristics for different excitation intensities.

Also, it can be noticed that the stiffness is not sensitive to frequency changes especially at low frequencies. This is attributed to the fact that at low frequency the dynamic stiffness of pile is quite close to the static one. However, the damping coefficient of piles rapidly increases as the frequency approaches zero, as a result of converting the soil material damping to the frequency-dependent equivalent viscous damping

coefficient, *c*. For calculated curves using the nonlinear approach in case of helical pile, it can be concluded that the stiffness decreases with increasing excitation intensity; however, stiffness remains almost constant over the range of applied excitation for the case of driven pile. This stems from the observation that the only case which has obvious nonlinearity in response is helical pile.

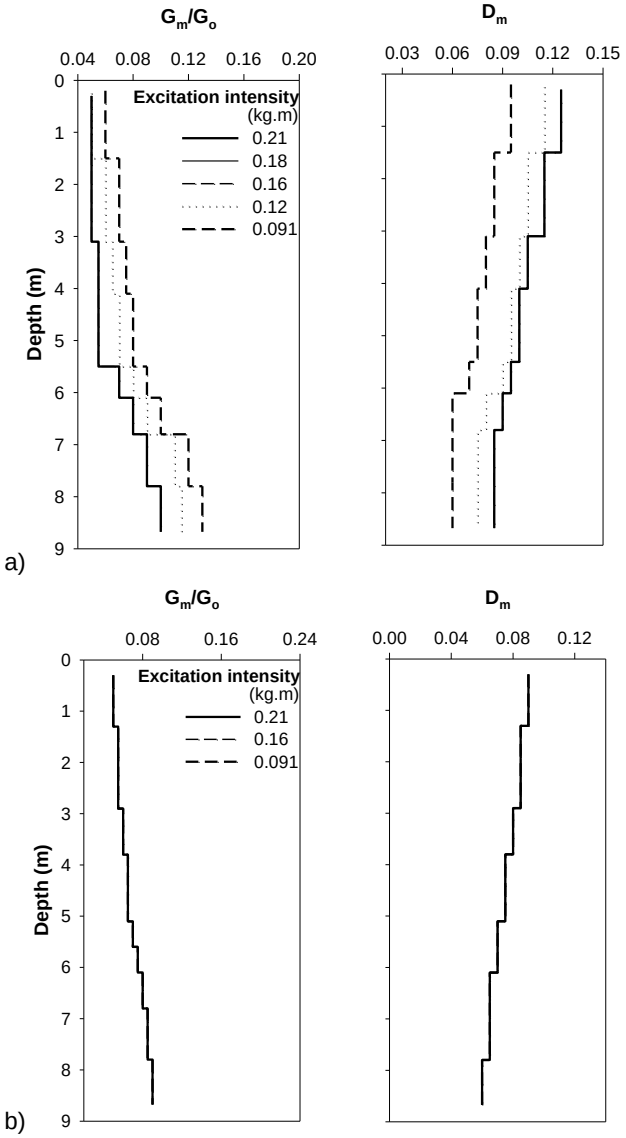

Figure 6. Distribution of weak zone shear modulus ratio and damping ratio: a) helical pile and b) driven pile

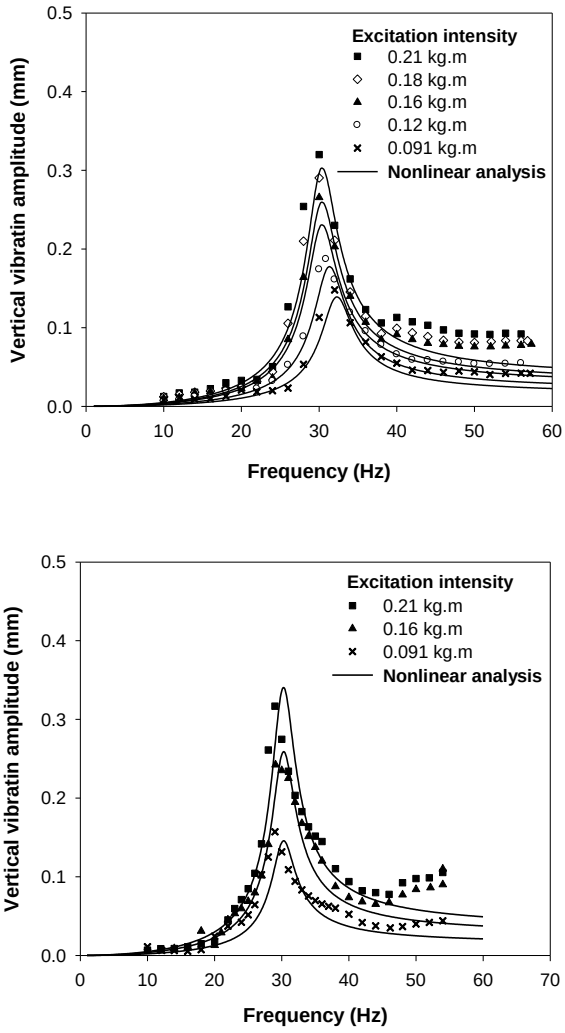

Figure 7. Experimental versus linear approach response curves: a) helical pile and b) driven pile

8 CONCLUSIONS

This study involved the in-situ dynamic performance of full-scale helical and driven piles and the validation of the theoretical formulations in matching the field response curves and estimating the impedance parameters of piles. The field tests included a closed-ended single-helix large diameter helical pile of 9.0 m long, 0.324 m shaft diameter, and 0.61 m helix diameter and a closed-ended driven steel-pipe pile with same length and diameter, installed in typical Alberta, Canada soils. Several tests with different excitation intensities were performed. Two different theoretical approaches, namely: linear and nonlinear approaches, incorporated in the program DYNA 5, were employed. Based on the experimental and analytical results obtained in this study, the following conclusions can be drawn:

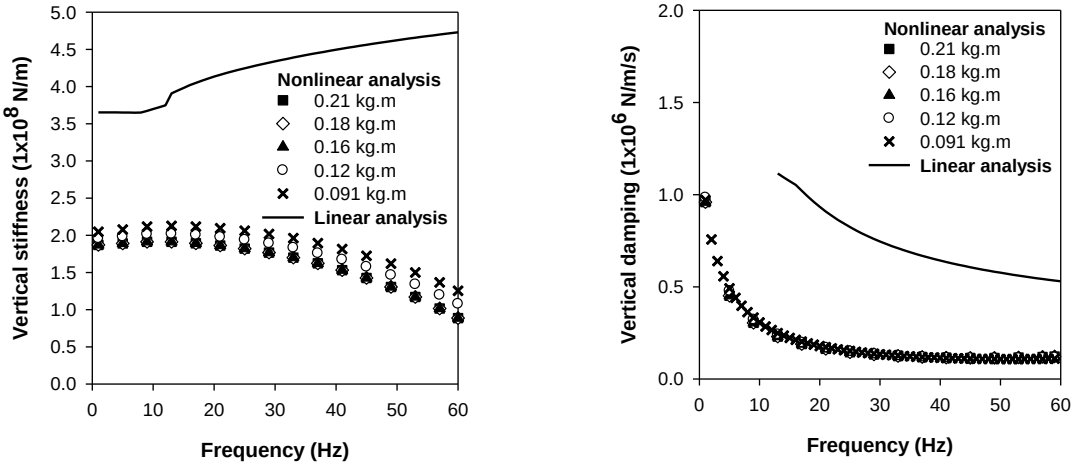

Figure 8. Stiffness and damping of helical pile

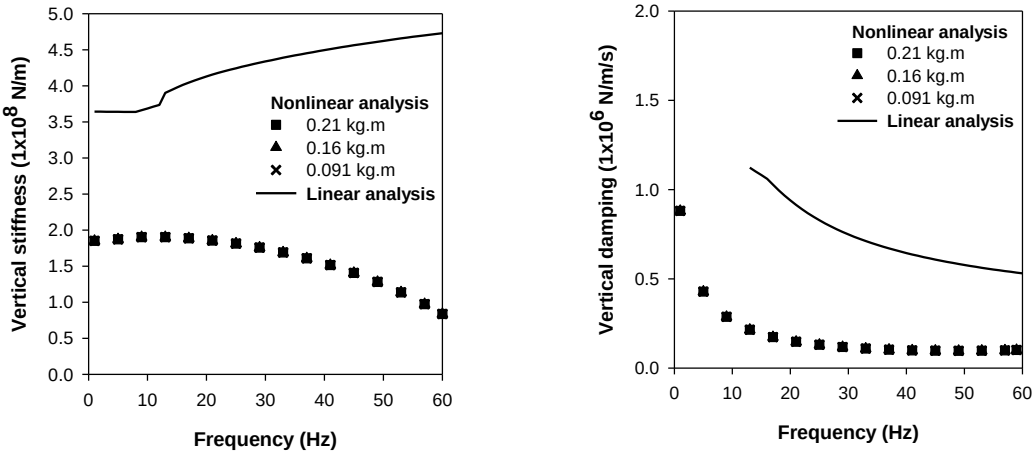

Figure 9. Stiffness and damping of driven pile

1. The measured responses of the driven pile were significantly close to those of the helical pile. This points out to conclusion that the performance characteristics of large-capacity helical piles are similar to those of steel driven piles for the piles' geometry considered in this study.
2. The linear analysis highly overestimated both the stiffness and damping of piles due to the assumed perfect bonding between pile and soil.
3. The nonlinear approach provided a reasonable estimation for piles' response curves and impedance parameters. Such agreement, confirmed the influence of soil disturbance due to pile installation process on the dynamic response of helical and driven piles.
4. The pile-soil separation length predicted by the nonlinear approach for the test piles varied between 1.54 and 1.85 times the shaft radius for the levels of dynamic excitation considered in this study.

9 ACKNOWLEDGEMENTS

The research described herein received direct support from the Natural Sciences and Engineering Research Council of Canada, University of Western Ontario, and ALMITA Manufacturing Ltd, Canada.

10 REFERENCES

Adams, J.I. and Klym, T.W. 1972. A Study of Anchorages for Transmission Tower Foundations, *Canadian Geotechnical J.*, 9(1): 89-104.

Baranov, V.A. 1967. On the calculation of excited vibrations of an embedded foundation, *Voprosy Dinamiki Prochnocti*, No. 14, Polytech. Institute Riga: 195-209.

Blaney, G.W., Muster, G.L., and O'Neill, M.W. 1987. Vertical vibration test of a full-scale pile group, *Proc. of Dynamic Response of Pile Foundations -*

Experiment, Analysis, and Observation, Geotechnical special publication No. 11, ASCE: 149-165.

Bobbitt, D.E. and Clemence, S.P. 1987. Helical Anchors: Application and Design Criteria, *Proc. of the 9th Southeast Asian Geotech. Conf.*, Bangkok, Thailand: 6-105 to 6-120.

Carville, C.A. and Walton, R.W. 1995. Foundation Repair using Helical Screw Anchors, *Foundation Upgrading and Repair for Infrastructure Improvement*, Edited by William F. Kane and John M. Tehaney, Geotechnical Special Publication No. 50, ASCE, San Deigo, California: 56-75.

Elkasabgy, M., El Naggar, M.H., and Sakr, M. 2010. Full-scale vertical and horizontal dynamic testing of a double helix screw pile, *Proc. of the 63rd Canadian Geotech. Conf.*, Calgary, Canada: 352-359.

El-Marsafawi, H., Han, Y.C. and Novak, M. 1992. Dynamic Experiments on Two Pile Groups, *J. of Geotechnical Engineering Division*, ASCE, 118(4): 576-592.

El Naggar, M.H., Novak, M., Sheta, M., El Hifnawi, L., and El Marsafawi, H. 2011. *DYNA 6 - a computer program for calculation of foundation response to dynamic loads*. Geotechnical Research Centre, The University of Western Ontario, London, Ontario, Canada.

El Naggar, M.H., Shayanfar, M.A., Kimiaei, M., and Aghakouchak, A.A. 2005. Simplified BNWF model for nonlinear seismic response analysis of offshore piles with nonlinear input ground motion analysis, *Canadian Geotechnical J.*, 42(2): 365-380.

El Naggar, M.H. and Abdelghany, Y. 2007a. Seismic Helical Screw Foundations Systems, *Proc. of the 60th Canadian Geotech. Conf.*, Ottawa, Ontario, Canada: 21-24.

El Naggar, M.H. and Abdelghany, Y. 2007b. Helical Screw Piles (HSP) Capacity for Axial Cyclic Loadings in Cohesive Soils, *Proc. of the 4th International Conf. on Earthquake Geotechnical Engineering*, Thessaloniki, Greece: 25-28.

El Sharnouby, B. and Novak, M. 1984. Dynamic experiments with group of piles, *J. of Geotechnical Engineering*, ASCE, 110(6): 719-737.

Kuhlemeyer, R.L. 1979. Vertical vibration of pile, *J. of Geotechnical Engineering Division*, ASCE, 105(2): 273-287.

Manna, B. and Baidya, D.K. 2009. Vertical vibration of full-scale pile - analytical and experimental study, *J. of Geotechnical and Geoenvironmental Engineering*, ASCE, 135(10): 1452-1461.

Nogami, T. and Novak, M. 1976. Soil-pile interaction in vertical vibration, *International J. of Earthquake Engineering and Structural Dynamics*, 4: 277-293.

Novak, M. 1974. Dynamic stiffness and damping of piles, *Canadian Geotechnical J.*, 11(4): 574-598.

Novak, M. and Grigg, R. 1976. Dynamic experiments with small pile foundations, *Canadian Geotechnical J.*, 13(4): 372-385.

Novak, M. 1977. Vertical vibration of floating piles, *J. of the Engineering Mechanics Division*, ASCE, 103(EM1): 153-168.

Novak, M. and Aboul-Ella, F. 1978a. Impedance functions for piles embedded in layered medium, *J. of Engineering Mechanics*, ASCE, 104(33): 643-661.

Novak, M. and Aboul-Ella, F. 1978b. Stiffness and damping of piles in layered media, *Proc. of Earthquake Engineering and Soil Dynamics*, ASCE, Specialty Conference, Pasadena, California: 704-719.

Novak, M., Nogami, T., and Aboul-Ella, F. 1978. Dynamic soil reactions for plane strain case, *J. of Engineering Mechanics*, ASCE, 104(EM4): 953-959.

Novak, M. and Sheta, M. 1980. Approximate approach to contact problems of piles, *Proc. of Dynamics Response of Pile Foundations: Analytical Aspects*, ASCE, New York: 53-79.

Novak, M. and El Sharnouby, B. 1983. Stiffness constants of single piles, *J. of Geotechnical Engineering*, ASCE, 109(7): 961-974.

O'Neill, M. 2001 Side resistance in piles and drilled shafts, *J. of Geotechnical and Geoenvironmental Engineering*, ASCE, 127(1): 3-16.

Penzien, J. 1970. *Soil-pile foundation interaction*, *In Earthquake Engineering*. New Jersey: Prentice-Hall Inc.

Randolph, M.F., Carter, J.P., and Wroth, C.P. 1979. Driven piles in clay-the effects of installation and subsequent consolidation, *Géotechnique*, 29(4): 361-393.

Sakr, M. 2009. Performance of helical piles in oil sand, *Canadian Geotechnical J.*, 46(9): 1046-1061.

Sheta, M. and Novak, M. 1982. Vertical vibration of pile groups, *J. of Geotechnical Engineering Division*, ASCE, 108(4): 570-590.

Veletsos, A.S. and Verbic, b. 1973. Vibration of viscoelastic foundations, *Earthquake Engineering and Structural Dynamics*, 2(1): 87-102.

Wolf, J.P., Meek, J.W., and Song, C. 1992. Cone models for a pile foundation, *In Piles under Dynamic Loads*, Geotechnical Special Publication No. 34, ASCE: 94-113.

Zhang, D.J.Y. 1999. *Predicting Capacity of Helical Screw Piles in Alberta Soils*, M.E.Sc. Thesis, University of Alberta, Edmonton, AB.